Physical controls of variability in North Atlantic phytoplankton communities

Andrew D. Barton,[a,b*] M. Susan Lozier,[a] and Richard G. Williams[b]

[a]Earth and Ocean Sciences, Nicholas School of the Environment, Duke University, Durham, NC

[b]Department of Earth, Ocean and Ecological Sciences, School of Environmental Sciences, University of Liverpool, Liverpool, United Kingdom

*Corresponding author: andrew.barton@duke.edu

Running head: North Atlantic phytoplankton community variability

Acknowledgements

We thank: David Johns and the Sir Alister Hardy Foundation for Ocean Science for maintaining and providing the Continuous Plankton Recorder data used in this study; Doug Smith of the UK MetOffice for providing the gridded temperature and salinity data; the National Centers for Environmental Prediction and National Center for Atmospheric Research (NCEP/NCAR) for providing the heat flux and wind data. ADB was supported by the NSF International Research Fellowship Program; MSL was supported by the Ocean Biology and Biogeochemistry Program at the National Aeronautics and Space Administration; RGW was supported by the UK Natural Environment Research Council (NE/H02087X/1).

Abstract

The structure of marine phytoplankton communities in the North Atlantic Ocean varies considerably on seasonal, interannual, and longer timescales in response to environmental change. However, the causes of ecological variability on interannual and longer timescales remain uncertain. Here, using a half-century of observations, we compare changes in atmospheric forcing (surface wind speed and heat fluxes) and ocean surface properties (sea surface temperature, mixed layer depth, thermal stratification, and turbulent kinetic energy) with variability in total phytoplankton biomass and the abundances of diatoms and dinoflagellates, as measured by the Continuous Plankton Recorder survey. On seasonal timescales, there is a clear connection between observed changes in the physical environment and the phytoplankton assemblages. Strong turbulence, deep mixed layer depths, and weak stratification decrease diatom abundance in the subpolar gyre, but increase diatoms in the subtropical gyre, a pattern broadly consistent with growth limitation of phytoplankton in high and low latitudes by light and nutrients, respectively. In contrast, dinoflagellates prosper in stratified, weakly turbulent conditions in sampled portions of the subpolar and subtropical gyres. On interannual to multidecadal timescales, however, the links between observed ecological and physical changes are much weaker. The physical mechanisms that differentiate the fates of diatoms and dinoflagellates on seasonal timescales do not appear to control their longer-term variability, perhaps because year-to-year variability in the phytoplankton assemblages is greater than in the physical drivers. This suggests that other biological (e.g., zooplankton grazing, chaos in the plankton) or physical mechanisms (e.g., changes in ocean circulation) may play important, regulatory roles.

Introduction

The structure of North Atlantic phytoplankton communities varies in response to changes in ocean surface conditions and atmospheric forcing (Sverdrup 1953; Margalef 1978; Taylor et al. 1993). These ecological changes are important because they have the potential to affect the broader marine food web, global biogeochemical cycles, and the climate system (Falkowski et al. 1998; Henson et al. 2012). While the physical drivers of seasonal changes in North Atlantic phytoplankton communities are relatively well-studied (Sverdrup 1953; Follows and Dutkiewicz 2002), if still debated (Behrenfeld 2010; Taylor and Ferrari 2011), considerably less is known about how and why phytoplankton communities have varied on interannual to multidecadal timescales. Do the same physical mechanisms that guide seasonal ecological change govern ecological variability on longer timescales? In particular, how do subtropical and subpolar gyre communities and distinct phytoplankton assemblages, such as diatoms and dinoflagellates, respond to the physical forcing?

To address these questions, we examine and compare a half-century of concomitant phytoplankton assemblage, atmospheric forcing, and surface oceanographic observations taken in the subtropical and subpolar North Atlantic. The Continuous Plankton Recorder (CPR) survey has sampled greater than 100 common diatom and dinoflagellate species over the North Atlantic subpolar and northern subtropical gyres since 1958, and provides an internally-consistent and unparalleled view of surface ecological variability (Richardson et al. 2006). Though the CPR data have known limitations associated with sampling procedures (e.g., Richardson et al. 2006; Barton et al. 2013), they offer temporal, spatial, and taxonomic coverage not possible with any other dataset, and therefore offer a unique and crucial perspective of how marine phytoplankton assemblages shift through time and space (Edwards and Richardson 2004; Leterme et al. 2005;

Hinder et al. 2012). We consider long-term records of phytoplankton color index (PCI), a proxy for total surface phytoplankton biomass, and the total abundances of diatoms and dinoflagellates, two key phytoplankton functional groups with strongly contrasting ecological niches and contributions to marine biogeochemical cycles (Cushing 1989; Henson et al. 2012; Irwin et al. 2012). By decomposing the observed ecological variability into seasonal, interannual to multidecadal (variations longer than one year, but less than the ~50-year long record), and a long-term trend component (comparable to the ~50-year record), we assess which physical mechanisms act as key drivers at each timescale, their regional relevance, and their importance to diatom and dinoflagellate abundance. The primary physical drivers that are believed to shape phytoplankton community structure include mechanical forcing and surface buoyancy fluxes from the atmosphere, which then alter the physical environment (turbulent kinetic energy in the mixed layer, sea surface temperature, mixed layer depth, and upper water column stratification). These key physical drivers potentially impact the light and nutrients experienced by phytoplankton in the ocean surface (Sverdrup 1953; Follows and Dutkiewicz 2002), but also the interactions and imbalances between predators and prey (Behrenfeld 2010; Behrenfeld and Boss 2014). The goal of our analysis is to evaluate and assess the statistical links between each phytoplankton metric (PCI, abundance of diatom and dinoflagellates) and likely physical drivers for different timescales across the northern subtropical and subpolar North Atlantic Ocean.

Contrasting dynamics and habitats in subpolar and subtropical gyres

The CPR survey covers portions of the North Atlantic subpolar and subtropical gyres, and allows the environmental controls of phytoplankton assemblages to be assessed in a consistent manner. Here we highlight key differences between the gyres, in terms of circulation, nutrient

supply, and light availability, as the contrasts provide a guiding framework for interpreting the results of our study.

In the subtropical North Atlantic, prevailing surface wind stress patterns drive Ekman downwelling and deepen the nutricline (Fig. 1). The water column is stably stratified, and aside from entrainment due to seasonal or episodic mixing events and horizontal transports of nutrients (Williams and Follows 1998; Williams et al. 2000; Palter and Lozier 2008), the supply of nutrients to the surface euphotic zone is weak. Though light is generally abundant at these latitudes, the limited supply of nutrients leads to low phytoplankton biomass and to assemblages dominated by picoplankton and flagellates, with larger cells such as diatoms being relatively scarce (Tarran et al. 2006; Uitz et al. 2006; Ward et al. 2012). Population growth by photoautotrophs is typically balanced by grazing (Lessard and Murrell 1998; Landry et al. 2000), and much of the primary production in the ocean surface is fueled by nutrients remineralized locally within the surface layer (Azam et al. 1983).

In these relatively stratified waters, seasonality in atmospheric forcing mediates the entrainment flux of nutrients (Fig. 1B) and leads to changes in the phytoplankton community. For example, at the Bermuda Atlantic Time Series station (BATS; 31°50’ N, 64°10’ W) and the European Station for Time-series in the Ocean, Canary Islands (ESTOC; 29°10’ N, 15°30’ W), located on opposite sides of the North Atlantic gyre but at similar latitudes, increased surface winds and cooling in winter drive deeper mixing and entrainment of nutrients, spurring a contemporary surface increase in chlorophyll and primary production (Menzel and Rhyther 1960; Steinberg et al. 2001; Neuer et al. 2002). Weaker winds and surface warming in spring and summer restratify the water column, leading to lower primary production at the surface. In accord with this view, Follows and Dutkiewicz (2002) found that spatial variations in the

129 strength of the winter/spring bloom in the subtropical region within a given year are positively
130 correlated with the magnitude of turbulent kinetic energy inputs by wind mixing and surface
131 cooling.

132 In contrast to the subtropics, the prevailing winds over the subpolar North Atlantic drive
133 Ekman upwelling, making deep nutrients relatively accessible to phytoplankton (Fig. 1). Strong
134 winds and surface cooling in winter deepen the mixed layer and entrain nutrients to the surface,
135 whereas during summer the supply is generally weaker due to increased stratification (Williams
136 et al. 2000). In addition, surface nutrients here are augmented by seasonal induction of nutrients
137 from the nutricline (Williams et al. 2006). At this latitude, however, light supply is highly
138 seasonal and limits phytoplankton growth in winter. With abundant nutrients, ample light, and
139 weak grazing pressure in late winter, spring, or early summer, phytoplankton populations grow
140 rapidly (Sverdrup 1953; Behrenfeld 2010; Taylor and Ferrari 2011), but ultimately decline as
141 nutrients are exhausted, cells aggregate, die, or sink from the water column, and predators graze
142 down phytoplankton (Sarthou et al. 2005). Follows and Dutkiewicz (2002) found that spatial
143 variations in the strength of the spring or summer bloom in the subpolar region are negatively
144 correlated with the magnitude of turbulent kinetic energy inputs by wind mixing and surface
145 cooling. While larger phytoplankton cells and their predators are conspicuous features of
146 subpolar bloom conditions (Irigoien et al. 2004; Ward et al. 2012), relatively small cells and
147 flagellates, but fewer large cells, dominate stratified summer conditions (Barton et al. 2013).

148 The precise mechanisms that lead to the dramatic subpolar phytoplankton bloom have been
149 the subject of renewed interest. The traditional view, termed the critical depth hypothesis, holds
150 that phytoplankton bloom in spring as the mixed layer depth shoals above the critical depth, the
151 depth at which phytoplankton net growth becomes positive (Sverdrup 1953). Two recent studies

have extended this idea to differentiate between the depth of the mixed layer and the depth of active mixing, as defined by local wind and buoyancy forcing (Taylor and Ferrari 2011; Brody and Lozier 2014). The depth of active mixing can be much shallower than the mixed layer, implying that phytoplankton can bloom near the surface even when the mixed layer is still deep. An intriguing alternative to these "bottom up" perspectives places greater emphasis on the "top down" regulatory role of zooplankton grazing, and is termed the disturbance-recovery hypothesis (Behrenfeld 2010; Behrenfeld and Boss 2014). In this view, it is the decoupling of predator and prey mediated by physical disturbance and differential generation lengths, rather than light and nutrient availability, that primarily underpins seasonal changes in the phytoplankton. Though the sparsely sampled and coarsely resolved CPR data are not ideally suited for understanding the timing and initiation of spring blooms, to the extent that is possible we will look for evidence of these mechanisms in the North Atlantic CPR data.

Methods

Analysis of CPR data

We calculate a monthly mean Phytoplankton Color Index (PCI) for the years 1958-2006, using all available raw CPR tow data within each 2.5°x2.5° grid in our study domain. The PCI is a proxy for total phytoplankton biomass, and has been found to compare favorably with satellite-derived estimates of chlorophyll-a (Raitsos et al. 2005). We also calculate monthly mean integrated diatom and dinoflagellate abundance by summing the abundances of all surveyed diatom and dinoflagellate taxa that have been sampled consistently over the whole period (for a list of taxa, see Barton *et al.* 2013a). The integrated diatom and dinoflagellate abundance includes many, but not all, taxa within each group, and the PCI reflects all phytoplankton captured in the CPR mesh, not just diatoms and dinoflagellates. We use the term "assemblage" when referring to a subset of all phytoplankton species. The density of data samples varies in time and space, with the greatest number of samples taken in the northeast North Atlantic and along shipping routes (Fig. 2). Beyond the monthly averaging and spatial re-gridding, we deliberately have not smoothed or gap-filled any of the time series data in order to retain faithfully the character of the original, raw data. We have also conducted our analyses with data gridded to 1.25° and 5.0° resolution, and find the study results insensitive to this resolution choice. The 2.5° resolution is a compromise between having enough data in each grid cell for meaningful statistics and retaining resolution.

A simple framework is next outlined for decomposing variability in the phytoplankton time series at each grid cell into a range of different timescales, from seasonal to multidecadal. The noise associated with the CPR survey sampling is estimated and signal-to-noise ratios (SNR), which compare variance in phytoplankton and noise time series, are calculated. Our

187 approach is demonstrated with PCI data from the western English Channel, a relatively well-
188 sampled region (Fig. 3).

189 At a given location and time *t,* the observed phytoplankton data, P_t, can be decomposed
190 into a climatological mean seasonal cycle (P_t^{Season}), a long term trend (P_t^{Trend}), phytoplankton
191 variability on interannual to multidecadal timescales (P_t^{Var}), and sampling noise (P_t^{Noise}):

192 $$P_t = P_t^{Season} + P_t^{Trend} + P_t^{Var} + P_t^{Noise} \quad (1)$$

193 The climatological seasonal cycle, P_t^{Season}, is the mean of all available data, P_t, for a given grid
194 cell for a given month of the year (Fig. 3A, inset). The seasonal cycle is subtracted from P_t to
195 yield monthly anomalies, P_t' (Fig. 3B), from which we calculate the long-term trend, P_t^{Trend}
196 (Fig. 3B). The linear trend over the record is estimated using the non-parametric Theil-Sen
197 approach, which reduces the sensitivity to large outliers (Theil 1950; Sen 1968), a common
198 feature in the anomaly time series. P_t^{Var} is the residual after subtracting P_t^{Trend} from the monthly
199 anomalies, P_t', and includes ecological variability on interannual to multidecadal timescales.
200 Only significant ($p < 0.05$), non-zero trends are subtracted when calculating P_t^{Var}. We also
201 examined log-transformed CPR time series, but found the final results did not differ appreciably
202 from the non-log-transformed data.

203 Lastly, the signal to noise ratio (SNR) for each phytoplankton time series is calculated in
204 order to assess whether observed variability in the phytoplankton time series exceeds what might
205 occur from variable sampling density. Our approach here assumes that measurement errors in the
206 CPR survey are random and small and that errors in the CPR time series are associated with
207 sampling intensity. To estimate the sampling noise at time *t*, P_t^{Noise}, the standard error of all
208 available raw data is calculated within each grid cell for each month during 1958-2006. A
209 synthetic time series of noise is generated, and repeated 10,000 times, by multiplying the

standard error by a randomly generated Gaussian white noise time series (with a mean of zero and standard deviation of one). The SNR is calculated as the variance in each phytoplankton time series divided by the variance in the noise time series, $\sigma_{Phy}^2/\sigma_{Noise}^2$ (Fleming 2010). At each location, σ_{Phy}^2 is the variance in each phytoplankton time series—P_t^{Season}, P_t^{Trend}, and P_t^{Var}—and σ_{Noise}^2 is the mean variance of 10,000 randomly generated noise time series. A large SNR (SNR > 1) indicates that the variability in the phytoplankton time series is not likely a product of potential sampling biases.

Analysis of environmental data

The physical data for the North Atlantic basin are similarly decomposed using the framework (1), including surface wind speed (m s^{-1}), total heat flux (H; H>0 for fluxes out of the ocean; W m^{-2}), depth-integrated turbulent kinetic energy (TKE) generation in the surface boundary layer (m^3 s^{-3}), sea surface temperature (SST; °C), stratification (°C), and mixed layer depth (MLD; m). The SST is the temperature in the surface layer (0-10m depth) obtained from the UK Met Office temperature and salinity reanalysis data set (Smith and Murphy 2007), which combines historical and more recent Argo measurements of temperature and salinity with model covariance fields to produce a gap-free global data set. Stratification is evaluated from the difference in temperature between the surface and 200 meters, again using the temperature reanalysis data. The mixed layer depth is diagnosed using a potential density threshold method (De Boyer Montégut et al. 2004), where the MLD is defined as the depth at which the potential density changes by 0.03 kg m^{-3} from the surface layer. Potential density profiles were calculated from UK Met Office reanalysis temperature and salinity data.

Sea surface wind and air-sea heat fluxes are taken from monthly mean NCEP/NCAR reanalysis data (Kalnay et al. 1996), and we have summed latent, sensible, longwave, and shortwave heat fluxes to get the total, net heat flux. Local mechanical forcing from the wind and penetrative convection from surface cooling generate TKE in the surface boundary layer, some of which is converted to potential energy (PE) by deepening the mixed layer and increasing its density. The dominant terms in the TKE budget are diagnosed following Niiler and Kraus (1977), and as applied by Follows and Dutkiewicz (2002):

$$\frac{dh}{dt} h\,\Delta b = m_1 u_*^3 + m_2 \frac{\alpha g h}{\rho C_p 2} H \quad (2)$$

where the rate of conversion of TKE to PE (first term) is sustained by the inputs of TKE from the wind (second term) and penetrative convection from surface cooling (third term); here Δb is the change in buoyancy between the mixed layer and the thermocline (m s^{-2}), g is gravity (m s^{-2}), α is the thermal expansion coefficient (K^{-1}), C_p is heat capacity of water (J kg^{-1} K^{-1}), h is mixed layer depth (m), u^* (m s^{-1}) is frictional wind velocity ($= \sqrt{|\vec{\tau}|/\rho}$), $\vec{\tau}$ is surface wind stress (N m^{-2}) from NCEP/NCAR monthly mean data, and ρ is density of seawater (kg m^{-3}). Coefficients m_1 and m_2 define the amount of energy available for mixing; m_1 is typically 1.25, whereas m_2 is approximately 1.0 during periods of surface warming and 0.15 in periods of surface cooling (Kraus 1988). Increasing TKE lowers the time-averaged light experienced by a phytoplankton cell, and is associated with entrainment of nutrients into the surface layer.

Finally, the connection between the ecosystem and physical variables is assessed using Kendall's τ coefficient, which is less sensitive to outliers than the more traditional Pearson correlation.

Results

Seasonal environmental change and biological responses

Our analysis confirms a cornerstone of biological oceanography: clear and widespread connections between seasonal cycles of key environmental drivers and seasonal cycles of total phytoplankton biomass and the abundance of diatoms and dinoflagellates in the North Atlantic (Margalef 1978; Taylor et al. 1993; Barton et al. 2013). Though these patterns have been previously described using a range of independent data sets, their robust signature and gyre-scale coherence lend confidence to the ability of the CPR survey to faithfully capture meaningful ecological patterns.

The seasonal analysis also highlights important differences in the mechanisms that regulate subtropical and subpolar PCI, as well as novel distinctions between the diatom and dinoflagellate assemblages. In the subpolar gyre, PCI is positively correlated with stratification and sea surface temperature, but negatively correlated with surface wind stress, heat flux, TKE, and mixed layer depth (Figs. 4A). In contrast, in the subtropical gyre, PCI is negatively correlated with stratification and sea surface temperature, but positively correlated with surface wind stress, heat flux, TKE, and mixed layer depth (Figs. 4A). Diatoms exhibit seasonal correlations with physical drivers that are similar to the total phytoplankton biomass (Figs. 4B). Dinoflagellates, by contrast, exhibit seasonal responses to physical drivers that are distinct from the total biomass and diatom abundance (Fig. 4C). Across the subpolar and subtropical gyres, dinoflagellates prosper during warm, stratified conditions, and their abundance is negatively correlated with surface wind speed, cooling, turbulence, and deeper mixed layers.

We provide additional context for these correlations by showing the climatological seasonal cycles of PCI, diatom abundance, dinoflagellate abundance, and mixed layer depth

(with scale inverted to show negative depths) for a subtropical and subpolar location (Fig. 5). In the northern subtropical location (Fig. 5A), mixed layers are relatively shallow but still seasonally variable, reaching a maximum depth in February. PCI peaks in May, but there is a robust fall bloom in this area, unlike the subpolar location. Diatoms bloom early in spring (March), decline through the summer, and show a very weak fall bloom. Dinoflagellates are generally more abundant in warm season months, with maxima in May and July-August. Interestingly, the fall PCI bloom does not appear to be primarily driven by changes in diatom or dinoflagellate populations, implying that other taxa (e.g., small but captured cells, taxonomic groups and species not sampled by the CPR survey or considered in this study) are responsible for the peak in PCI here. In the subpolar location (Fig. 5B), mixed layers are deepest in March, shoal rapidly through early summer, and then deepen again through late summer and fall. There is a robust spring bloom peaking in June and much more modest fall bloom of diatoms and PCI peaking in September. Dinoflagellates are most abundant in summer, with a maximum in July. These seasonal cycles of total biomass, diatoms, and dinoflagellates are broadly consistent with previous CPR studies (Barton et al. 2013) and satellite observations (D'ortenzio et al. 2012; Taboada and Anadon 2014).

Multidecadal trends

Between 1958 and 2006, phytoplankton biomass increased over a swath of the subpolar North Atlantic (Fig. 6A), a pattern that has been previously reported and linked to climate variability (Barton et al. 2003). A few isolated areas exhibited a decline in PCI, but for most areas there has been no significant trend. The abundances of diatoms and dinoflagellates have decreased in the northeast Atlantic, but have not significantly changed elsewhere (Fig. 6A).

Hinder et al. (2012), sampling only the most common taxa in this region, reported a strong decline of dinoflagellates, but little change in diatoms. The contrast in the northeast Atlantic between increasing PCI but decreasing diatoms and dinoflagellates is striking, as it is generally believed that periods and places with greater chlorophyll or biomass also have proportionally more large phytoplankton cells, such as diatoms and dinoflagellates (Chisholm 1992; Irigoien et al. 2005). It is also interesting that the increase in PCI in the central North Atlantic does not appear to be driven by an increase in diatoms or dinoflagellates. The mismatch between PCI and diatom and dinoflagellate assemblage trends implies that other types of phytoplankton are varying independently from diatoms and dinoflagellates. However, the CPR survey does not fully resolve these other taxa.

During this same period, there has been a long-term increase in wind speed over the central subpolar gyre, the North Sea, and northeast Atlantic, with a decline in waters off of Spain and North Africa (Fig. 6B). Surface heat loss increased along the path of the Gulf Stream and North Atlantic Current, with some enhanced heat input elsewhere (recall that $H>0$ implies a flux out of the ocean). Trends in mixed layer TKE have less spatial coherence, but there is an area of decreasing turbulence near Spain and North Africa (Fig. 6B), in the same vicinity as the weakened winds. SST in much of the subtropical and subpolar North Atlantic has warmed strongly, yet much of the region of increasing PCI has not shown significant surface warming (Fig. 6C). These SST trends are consistent with other observational studies (Deser et al. 2010). At the same time, mixed layers have deepened in waters near Greenland and Iceland, but have shoaled in the central North Atlantic on the inter-gyre margin and in the northeast Atlantic near Europe (Fig. 6C). The spatial pattern of trends for stratification is nearly the reverse, with decreased stratification in the Labrador Sea and near Greenland, but increased stratification in

the central and northeast North Atlantic (Fig. 6C). While it is impossible to rule out or prove a connection between slow-moving environmental and ecological change based upon these data alone, none of the long-term trends in atmospheric forcing or ocean conditions examined here correspond closely to the spatial patterns seen in the multidecadal biological trends.

Interannual to multidecadal variability

Though there is strong correlation between observed physical and PCI time series in the North Atlantic (Fig. 7A), this correlation is largely a consequence of seasonal variations (Fig. 7B). After the seasonal cycles (e.g., Figs. 4) and linear trends (e.g., Fig. 6) have been removed from PCI time series, there is little connection between ecological variability and physical forcing occurring on interannual to multidecadal timescales (Fig. 7C). A similar pattern is true for both diatoms and dinoflagellates (data not shown). The apparent insensitivity of the phytoplankton assemblages to interannual to multidecadal variability in the environment can be seen at a subtropical and subpolar location in the North Atlantic, where there is no correlation between PCI^{Var}, Dia^{Var}, $Dino^{Var}$ and MLD^{Var} (Fig. 8). For example, the phytoplankton assemblage in the subpolar North Atlantic (Fig. 8B) does not appear to track the deepening of the mixed layer from the 1970s to 1990s, associated with a change in NAO phase from negative to positive.

The lack of a clear connection between physical forcing and ecological change on interannual to multidecadal timescales, however, does not preclude significant ecological variability on these timescales. After subtracting the seasonal cycles and trends from the PCI time series, there is strong PCI variability that exceeds our estimates of sampling noise, as indicated by signal to noise ratios that are generally greater than one (Fig. 9; the same is true for

346 diatoms and dinoflagellates; data not shown). Thus, there is considerable variability occurring on
347 these timescales that is not easily or simply linked to the principal physical drivers considered in
348 this study. The variance in phytoplankton and physical time series at each timescale provides
349 further context for the lack of correlation: year-to-year variability in the plankton assemblage is
350 considerably greater than in the physical drivers (Table 1).

351 Our analyses focus on monthly relationships between atmospheric forcing and
352 oceanographic conditions and the phytoplankton assemblages. However, we have also
353 investigated whether environmental changes in winter could have subsequent ecological impacts
354 throughout the growing season. We find no widespread and robust correlation between the
355 maximum depth of winter mixing and the maximum (or the average) phytoplankton biomass
356 (PCI) throughout the growing season (defined here as January through August; data not shown).

357 We have also diagnosed the correlations between the NAO index (Hurrell 1995) and each
358 of the physical and ecological time series across the North Atlantic, using monthly time series
359 and the winter NAO index (December to March). There are strong and significant correlations
360 between the NAO and each of the physical variables considered in our study, as has been
361 reported elsewhere (Marshall et al. 2001). However, similar to Barton et al. (2003), we find no
362 widespread, significant link between the winter NAO index and PCI or diatom and dinoflagellate
363 assemblages (data not shown).

364

Discussion

In the following discussion, we first consider the empirical evidence for how atmospheric forcing and ocean surface conditions control phytoplankton assemblages on seasonal timescales, highlighting mechanistic differences in the behavior of the subpolar and subtropical gyres and the responses of diatoms and dinoflagellates. We then examine possible explanations for why there is no obvious link between physical and ecological change on interannual to multidecadal timescales in the North Atlantic, and discuss several key physical and biological processes that may play important, and as yet, unresolved roles.

Seasonal forcing of total phytoplankton biomass in subtropical and subpolar habitats

Our analysis broadly reaffirms the paradigm that the seasonal changes in phytoplankton biomass (PCI) in the subpolar and subtropical North Atlantic are constrained by the availability of light and nutrients, respectively, as mediated by seasonal changes in atmospheric forcing (Sverdrup 1953; Menzel and Rhyther 1960; Follows and Dutkiewicz 2002). In the subpolar gyre, strong winds, cooling, and deep mixing tend to decrease phytoplankton biomass, whereas stratification and warmer SSTs are correlated with increased phytoplankton biomass (Figs. 4-5). In the northern subtropical gyre, strong winds, cooling, and deep mixing lead to increased PCI, whereas stratification and warmer SSTs lead to decreased PCI (Fig. 4-5). In the northern subtropical regions covered by the CPR survey (Fig. 5A), there is also a robust autumn bloom driven by deepening mixed layers and entrainment of nutrients (Cushing 1959; Colebrook 1982).

The CPR data offer unique perspectives on the applicability of the "top-down" disturbance-recovery mechanism across contrasting ocean regimes. In the northern subtropical areas (Fig. 5A), phytoplankton bloom strongly in winter or spring while mixed layers are deepest, and

388 increase well in advance of the switch from cooling to heating at the ocean surface. Thus, we
389 argue that the best explanation for seasonal dynamics here is the seasonal entrainment of
390 nutrients, rather than the critical depth (Sverdrup 1953) or disturbance-recovery hypotheses
391 (Behrenfeld and Boss 2014). In subpolar seas, PCI begins increasing while the mixed layer is
392 deepest and light is still low (Fig. 5B), consistent with the disturbance-recovery hypothesis.
393 However, rapid shoaling of the mixed layer and a switch from cooling to warming the ocean
394 surface precede the period of greatest PCI increases in these latitudes (Fig. 5B), consistent with a
395 more traditional biophysical view of how subpolar spring phytoplankton blooms proceed
396 (Sverdrup 1953; Taylor and Ferrari 2011; Brody and Lozier 2014). However, we note that the
397 MLD may not be the appropriate metric for gauging phytoplankton exposure to light: Brody and
398 Lozier (2014) demonstrated that the depth of active mixing is shallower than the MLD prior to
399 the onset of stratification. Thus, though we find tentative support for both the critical depth
400 hypothesis and "top-down" disturbance-recovery mechanism in the subpolar North Atlantic, the
401 coarsely sampled and averaged CPR survey data and the lack of mixing length data preclude
402 further speculation on the precise triggers and timing of phytoplankton.
403
404 ***Contrasting seasonal responses of diatoms and dinoflagellates***
405 Diatoms and dinoflagellates are significant components of the phytoplankton community in
406 the North Atlantic, and have different life histories, physiologies, and trophic strategies (Smayda
407 1997; Sarthou et al. 2005). The traditional view of their ecology, formalized by Ramon
408 Margalef's mandala paradigm, holds that diatoms prefer turbulent, nutrient-rich conditions and
409 dinoflagellates calm, nutrient-poor conditions (Margalef 1978; Smayda and Reynolds 2001;
410 Irwin et al. 2012). Our present analysis and increasing knowledge of how diatom and

411 dinoflagellate traits determine their fitness under different environmental conditions (Ward et al.
412 2011; Irwin et al. 2012; Barton et al. 2013) allow us to update and refine this paradigm to
413 account for differences between subtropical and subpolar systems.

414 In the downwelling, nutrient-limited subtropical gyre, increasing turbulence and mixing
415 increases diatom abundance, as expected, whereas in the upwelling, light-limited subpolar gyre,
416 the opposite is generally true (Fig. 4). Diatoms are largely photoautotrophic, non-motile
417 phytoplankton that require silica to form their covering frustules. For a given cell size, diatoms
418 are able to grow relatively quickly, compared with other taxa, and have high affinities for nitrate
419 and phosphate (Litchman et al. 2007; Edwards et al. 2012). They can also tolerate low and
420 variable light conditions (Chan 1978; Depauw et al. 2012). These traits are thought to enable
421 diatoms to form conspicuous blooms in relatively turbulent, nutrient rich conditions at high
422 latitudes (Sieracki et al. 1993; Dale et al. 1999; Rynearson et al. 2013) and low latitude
423 upwelling systems in the North Atlantic (Taylor et al. 2012). However, where light may be
424 limiting, such as in the high latitudes in spring and winter, increasing turbulence may exacerbate
425 light limitation. Thus, while pulses of nutrients (Schartau et al. 2010) and increased uptake of
426 nutrients due to turbulence favor diatoms (Barton et al. 2014), and support classical Margalef's
427 mandala paradigm, we have shown here that this perspective should be refined on seasonal
428 timescales to be specific to the dynamics within each gyre.

429 The relationship between seasonal environmental change and dinoflagellate dynamics is
430 quite different from that of diatoms (Fig. 4). Generally speaking, diatom abundance peaks before
431 dinoflagellates in seasonal ecological succession (Barton et al. 2013). In both the subtropical and
432 subpolar gyres, strong winds, surface cooling, turbulence, and deep mixing are negatively
433 correlated with dinoflagellate abundance, whereas increasing stratification and SST coincide

434 with increases in dinoflagellate abundance. Dinoflagellates tend to have relatively low nutrient
435 affinities and growth rates (Litchman et al. 2007; Edwards et al. 2012), and are thus not generally
436 opportunistic bloom formers like diatoms (with the notable exception of harmful algal blooms;
437 Smayda 1997). Most, if not all, dinoflagellates are either mixotrophic (exhibiting both
438 photosynthetic and heterotrophic modes of nutrition) or heterotrophic (Stoecker 1999; Barton et
439 al. 2013). Mixotrophy is thought to be favored in resource poor conditions (Ward et al. 2011),
440 such as in stratified summer conditions in the North Atlantic. Heterotrophic dinoflagellates
441 appear to be most abundant during stratified summer conditions characterized by an abundance
442 of small prey cells (Barton et al. 2013). Finally, dinoflagellates are motile, yet their ability to
443 swim effectively to maximize exposure to light, nutrients, and prey is negatively impacted by
444 strong turbulence and shear (Durham et al. 2009), which may help explain the widespread
445 negative correlation with turbulence. Taken together, these traits help explain the strong and
446 basin-wide negative correlation of dinoflagellates with winds, cooling, turbulence, and mixing,
447 as well as the positive connection with stratification and SST (Fig. 4).
448 The strong contrasts between diatoms and dinoflagellates highlight an important point:
449 there is no single, universal mechanism that drives the seasonal cycles and blooms of all
450 phytoplankton species. Not only does the importance of different physical mechanisms vary
451 across the ocean and through time (e.g., Fig. 4), but the range of phytoplankton species traits and
452 complexity of predator-prey interactions implies that links between environmental forcing and
453 population change should be distinct for groups of similar phytoplankton. The seasonal
454 ecological succession of phytoplankton species in marine and freshwater systems illustrates the
455 complex variations present in the microbial community (Sommer 1985; Taylor et al. 1993), and

456 these patterns almost certainly cannot be explained without considering differences among
457 species, as we have highlighted here.
458
459
460 ***Ecological variability on interannual and longer timescales***
461 There is considerable variability in North Atlantic phytoplankton assemblages occurring on
462 interannual and longer timescales (Figs. 6-8, Table 1), yet it is not easily or directly linked to
463 variability in ocean surface wind speed, heat fluxes, turbulence, mixed layer depth, stratification,
464 or SST (Fig. 7). Though a linear response is not expected, we speculate that the lack of
465 sensitivity in the phytoplankton to long-term environmental variability may arise because the
466 year-to-year variability in the phytoplankton assemblages is greater than in the physical drivers
467 (Table 1). Our results for the North Atlantic do not preclude the possibility of particular
468 phytoplankton species (there are many species not sampled by the CPR survey, and we have
469 aggregated over many species), other functional groups (e.g., coccolithophores or picoplankton),
470 or specific regions being directly impacted by the physical variables that we have examined.
471 However, the lack of robust and widespread correlations between the usual physical drivers and
472 CPR-observed ecological variability suggests that the drivers of long-term ecological change in
473 the North Atlantic may be more complex and uncertain than previously reported. Here, we place
474 our results in the context of previous studies arguing for and against causal links from
475 atmospheric forcing and resulting ocean conditions to marine phytoplankton community
476 variability, and suggest other physical and biological mechanisms that may ultimately explain
477 the observed ecological variability in the North Atlantic.

In the subtropical North Atlantic, it has generally been argued that changes in local atmospheric forcing from year to year influence surface phytoplankton biomass and community structure. For example, in their analysis of in situ data from BATS (data from 1990-1996) and satellite chlorophyll data from 1998-2000 throughout the subtropical North Atlantic, Follows and Dutkiewicz (2002) found that years with stronger winds and surface cooling had stronger spring phytoplankton blooms. Several other satellite-based studies have found a decrease in spatially integrated subtropical primary production or an increase in the spatial extent of the oligotrophic regions (low chlorophyll), which they attributed to increasing water column stratification associated with warming of ocean surface waters (Behrenfeld et al. 2006; Polovina et al. 2008; Irwin and Oliver 2009). At BATS, interannual variability in primary productivity, total cholorophyll-a, and particulate carbon export are negatively correlated with the NAO index (Lomas et al. 2010), with positive NAO phases in this region being characterized by weaker winds and heat fluxes but higher surface temperatures (Bates 2001; Marshall et al. 2001). Though model studies indicate that changes in atmospheric forcing linked to contrasting states of the NAO should influence the vertical supply of nutrients at BATS (Oschlies 2001), it has proven difficult to explain how the NAO impacts the phytoplankton community at BATS. For example, the NAO and mixed layer depth do not appear to be significantly correlated at BATS (Lomas et al. 2010).

Moreover, several recent studies have not found a strong link between interannual variations in stratification and phytoplankton dynamics (Dave and Lozier 2010; Lozier et al. 2011; Dave and Lozier 2013). By pairing chlorophyll observations and primary production estimates with nearby hydrographic profiles throughout the oligotrophic regions of the global ocean, these studies have shown that phytoplankton variability is strongly linked to water column

501 stratification on seasonal timescales, yet there is to date no observed linkage between interannual
502 variations in subtropical phytoplankton communities and interannual variability in local
503 stratification. Instead, they argue that stratification changes to date may be insufficient to provide
504 this linkage and/or variations in broader scale oceanographic processes, such as Ekman and
505 geostrophic transports of nutrients, may help explain this variability (Williams and Follows
506 1998; Palter and Lozier 2008; Ayers and Lozier 2010). It is possible that the stratification-
507 phytoplankton link will become more apparent as climate warms in the coming century
508 (Steinacher et al. 2010; Bopp et al. 2013). However, our analysis of northern subtropical CPR
509 data supports these more recent studies questioning the direct link between local stratification
510 changes and phytoplankton dynamics observed in the North Atlantic subtropical region over the
511 past several decades.

512 In North Atlantic subpolar gyre, we also argue that the evidence for a link between local
513 atmospheric forcing and the phytoplankton assemblage variability occurring on interannual and
514 longer timescales is equivocal. Stronger surface winds and deeper mixed layers associated with
515 positive phases of the NAO have been found to favor diatoms over dinoflagellates in the pelagic
516 northeast North Atlantic, whereas dinoflagellates were more abundant in negative NAO
517 conditions, characterized by weaker winds and shallower mixed layers (Henson et al. 2012). In a
518 study of primarily continental shelf waters, Hinder et al. (2012) found a long-term increase in the
519 relative abundance of diatoms versus dinoflagellates, and linked this change to increases in wind
520 and sea surface temperature. Leterme et al. (2005) found that the winter NAO index was
521 positively correlated with PCI and diatom abundance in the central North Atlantic during the
522 spring bloom period (April-June), possibly in support of the hypothesis that deeper mixed layers
523 should favor diatoms (Henson et al. 2012).

However, it is unclear how broadly these processes apply throughout the subpolar gyre. For example, CPR data from the northeast Atlantic indicate a negative correlation between diatoms and the NAO index in May and a positive correlation between dinoflagellates and the NAO index in April and May (Leterme et al. 2005), seemingly in contrast with the mechanism outlined above for the central North Atlantic. Moreover, Follows and Dutkiewicz (2002) found no year-on-year connection between atmospheric forcing and satellite-measured surface chlorophyll concentration throughout the subpolar gyre or in observations from Ocean Weather Station ''India'' (59° N, 19° W). Much as within the subtropical gyre, these links may become clearer as the climate changes in the coming century (Steinacher et al. 2010; Bopp et al. 2013). Yet our analyses of historical observations imply that interannual variations in phytoplankton assemblages are not neatly explained by local atmospheric forcing and oceanographic conditions, suggesting that other mechanisms may have been important. But what might these mechanisms be? In the following, we speculate on the potential roles of ocean circulation, zooplankton predation, and chaos in the plankton assemblages, and suggest that testing the importance of each potential alternative explanation should be the subject of future research.

First, ocean circulation, including Ekman and geostrophic currents, has the capacity to impact surface phytoplankton communities by mediating the three-dimensional transport of nutrients. For example, along the northern flank of the subtropical gyre, strong winter winds generate a southward Ekman flux of subpolar nutrients into the subtropics (Williams and Follows 1998; Ayers and Lozier 2010). In the subpolar gyre, by contrast, horizontal Ekman fluxes generally remove nutrients from the euphotic zone. Because the winds across the North Atlantic are marked by spatially coordinated, low frequency variability (e.g., NAO), this mechanism may play a role in structuring phytoplankton communities on interannual to decadal

timescales, particularly at the intergyre boundary and margins. Geostrophic currents have also been shown to affect nutrient supply: geostrophic flow advects relatively nutrient-poor waters toward the subpolar gyre (Williams and Follows 1998; Williams et al. 2011), while nutrients are imported to the subtropical gyre via the upper limb of the meridional overturning circulation (Williams et al. 2006; Palter and Lozier 2008). Additionally, eddy mixing along the inter-gyre boundary has been shown to deliver nutrients from the subpolar to the subtropical basin (Bower et al. 1984). Therefore, interannual to decadal changes in the strength and geometry of the gyre circulations, as have been observed in the North Atlantic (Hakkinen and Rhines 2004; Hátún et al. 2005), are expected to impact the horizontal delivery of nutrients to the euphotic zone. Thus, we suggest that future studies of phytoplankton variability consider the ecological significance of broad scale changes in the three-dimensional ocean circulation.

Though our focus has been largely on "bottom-up" processes, zooplankton predation clearly plays an instrumental role in regulating phytoplankton assemblages. Mechanisms that disrupt the balance between predator and prey over longer timescales would make it more difficult to detect direct "bottom up" links between atmospheric and oceanographic forcing variability and phytoplankton assemblages. For example, growth rates of zooplankton and phytoplankton have different sensitivities to temperature (Eppley 1972; Rose and Caron 2007); many larger zooplankton, such as copepods, have multiple developmental stages and relatively long generation times that are dependent upon temperature (Kiørboe and Hirst 2008); and many zooplankton have overwintering strategies (e.g., diapause in copepods) or dormant phases (e.g., dinoflagellate cysts) that may be cued by environmental conditions (Hairston et al. 1990; Lee et al. 2006). Finally, as the environment changes through time, predator and prey species ranges and phenologies may change at different rates (Beaugrand et al. 2002; Edwards and Richardson

2004). Each of these mechanisms has the potential to alter the relative balance of top-down and bottom-up regulation of phytoplankton assemblages, yet our limited understanding of their impacts on long-term variability in phytoplankton assemblages precludes an assessment of their impact on the observations we report here (but see Chen et al. 2012; Calbet et al. 2014).

There is also growing appreciation of the importance of chaos in plankton communities, resulting possibly from resource competition or predator-prey dynamics (Beninca et al. 2008; Dakos et al. 2009; Kenitz et al. 2013). The presence of chaos, though still unsubstantiated in open ocean phytoplankton communities, would make detecting links between physical forcing and ecological change even more difficult.

Summary and Wider Implications

Large seasonal changes in atmospheric forcing and ocean surface conditions shape, to a great degree, the seasonal cycles of phytoplankton biomass, but also the relative abundance of phytoplankton species. These ecological changes in the phytoplankton are felt throughout the marine food web, and help define the strength and efficiency of the ocean's biological pump. At the same time, there are real variations in the North Atlantic phytoplankton assemblages occurring on interannual to multidecadal timescales. Explanations for this variability have often focused on longer-term variability in the same physical mechanisms (i.e., changes in atmospheric forcing and ocean surface conditions) that shape seasonal change in the phytoplankton community (Barton et al. 2003; Behrenfeld et al. 2006; Irwin and Oliver 2009).

Here, however, we have carefully examined a well-vetted, decades-long observational record of the subpolar and subtropical North Atlantic phytoplankton assemblage, and found that interannual to multidecadal changes in atmospheric forcing and surface oceanographic properties

593 do not clearly or simply explain the historical variations in the North Atlantic phytoplankton
594 assemblage. The lack of sensitivity in the phytoplankton to long-term variability in local
595 atmospheric forcing and ocean conditions may arise, in part, because the year-to-year variability
596 in the phytoplankton assemblage is much greater than in the physical drivers. It is also possible
597 that other ecological (e.g., zooplankton grazing, chaos in the plankton) and physical mechanisms
598 (e.g., ocean circulation) may play crucial, and as yet, poorly understood roles in driving observed
599 ecological changes. For example, several recent studies have considered how changes in ocean
600 circulation impact phytoplankton biomass or chlorophyll in the Pacific (Ayers and Lozier 2010;
601 Rykaczewski and Dunne 2010) and Atlantic Oceans (Hátún et al. 2009; Johnson et al. 2013), but
602 considerably uncertainty remains. Thus, our work indicates that the traditional "bottom up" view
603 that focused solely on local changes in atmospheric forcing and ocean conditions may not be
604 sufficient to understand how phytoplankton communities respond to changing climates, both in
605 the historical record and in anthropogenic climate change scenarios.
606
607
608

609 **References**
610
611 Ayers, J. M., and M. S. Lozier. 2010. Physical controls on the seasonal migration of the North
612 Pacific transition zone chlorophyll front. J. Geophys. Res. **115**, 10.1029/2009jc005596.
613 Azam, F., T. Fenchel, J. G. Field, J. S. Gray, L. A. Meyer-Reil, and T. F. Thingstad. 1983. The
614 ecological role of water-column microbes in the sea. Mar. Ecol. Prog. Ser. **10:** 257-263,
615 Barton, A. D., Z. V. Finkel, B. A. Ward, D. G. Johns, and M. J. Follows. 2013. On the roles of
616 cell size and trophic strategy in North Atlantic diatom and dinoflagellate communities.
617 Limnol. Oceanogr. **58:** 254-266, 10.4319/lo.2013.58.1.0254.
618 Barton, A. D., C. H. Greene, B. C. Monger, and A. J. Pershing. 2003. The Continuous Plankton
619 Recorder survey and the North Atlantic Oscillation: Interannual- to Multidecadal-scale
620 patterns of phytoplankton variability in the North Atlantic Ocean. Prog. Oceanogr. **58:**
621 337-358, 10.1016/j.pocean.2003.08.012.
622 Barton, A. D., B. A. Ward, R. G. Williams, and M. J. Follows. 2014. The impact of fine-scale
623 turbulence on phytoplankton community structure. Limnol. Oceanogr. Fluids Env. **4:** 34-
624 49, 10.1215/21573689-2651533.
625 Bates, N. R. 2001. Interannual variability of oceanic CO2 and biogeochemical properties in the
626 Western North Atlantic subtropical gyre. Deep. Sea. Res. **48:** 1507-1528,
627 Beaugrand, G., P. C. Reid, F. Ibanez, J. A. Lindley, and M. Edwards. 2002. Reorganization of
628 North Atlantic marine copepod biodiversity and climate. Science **296:** 1692-1694,
629 10.1126/science.1071329.
630 Behrenfeld, M. 2010. Abandonding Sverdrup's crtical depth hypothesis on phytoplankton
631 blooms. Ecology **91:** 977-989,
632 Behrenfeld, M. J., and E. S. Boss. 2014. Resurrecting the ecological underpinnings of ocean
633 plankton blooms. Ann. Rev. Mar. Sci. **6:** 167-194, 10.1146/annurev-marine-052913-
634 021325.
635 Behrenfeld, M. J. and others 2006. Climate-driven trends in contemporary ocean productivity.
636 Nature **444:** 752-755, 10.1038/nature05317.
637 Beninca, E. and others 2008. Chaos in a long-term experiment with a plankton community.
638 Nature **451:** 822-825, 10.1038/nature06512.
639 Bopp, L. and others 2013. Multiple stressors of ocean ecosystems in the 21st century: projections
640 with CMIP5 models. Biogeosci. Disc. **10:** 3627-3676, 10.5194/bgd-10-3627-2013.
641 Bower, A. S., H. T. Rossby, and J. L. Lillibridge. 1984. The Gulf Stream--Barrier or blender? J.
642 Phys. Oceanogr. **15:** 24-32,
643 Brody, S. R., and M. S. Lozier. 2014. Changes in dominant mixing length scales as a driver of
644 subpolar phytoplankton bloom initiation in the North Atlantic. Geophys. Res. Lett. **41:**
645 3197-3203, 10.1002/2014gl059707.
646 Calbet, A. and others 2014. Future climate scenarios for a coastal productive planktonic food
647 web resulting in microplankton phenology changes and decreased trophic transfer
648 efficiency. PloS One **9:** e94388, 10.1371/journal.pone.0094388.
649 Chan, A. 1978. Comparative physiological study of marine diatoms and dinoflagellates in
650 relation to irradiance and cell size. I. Growth under continuous light. J. Phycol. **14:** 395-
651 402,
652 Chen, B., M. R. Landry, B. Huang, and H. Liu. 2012. Does warming enhance the effect of
653 microzooplankton grazing on marine phytoplankton in the ocean? Limnol. Oceanogr. **57:**
654 519-526, 10.4319/lo.2012.57.2.0519.

Chisholm, S. W. 1992. Phytoplankton size. *In* P. G. Falkowski and A. D. Woodhead [eds.], Primary productivity and biogeochemical cycles in the sea. Plenum Press.
Colebrook, J. M. 1982. Continuous plankton records: seasonal variations in the distribution and abundance of plankton in the North Atlantic Ocean and the North Sea. J. Plankton. Res. **4:** 435-462,
Cushing, D. H. 1959. The seasonal variation in oceanic production as a problem in population dynamics. J. Cons. Int. Explor. Mer. **24:** 455-464,
---. 1989. A difference in structure between ecosystems in strongly stratified waters and in those that are weakly stratified. J. Plankton Res. **11:** 1-13,
D'Ortenzio, F., D. Antoine, E. Martinez, and M. Ribera d'Alcalà. 2012. Phenological changes of oceanic phytoplankton in the 1980s and 2000s as revealed by remotely sensed ocean-color observations. Glob. Biogeochem. Cyc. **26**, 10.1029/2011gb004269.
Dakos, V., E. Beninca, E. H. Van Nes, C. J. Philippart, M. Scheffer, and J. Huisman. 2009. Interannual variability in species composition explained as seasonally entrained chaos. Proc. Roy. Soc. Biol. Sci. **276:** 2871-2880, 10.1098/rspb.2009.0584.
Dale, T., F. Rey, and B. R. Heimdal. 1999. Seasonal development of phytoplankton at a high latitude oceanic site. Sarsia **84:** 419-435,
Dave, A. C., and M. S. Lozier. 2010. Local stratification control of marine productivity in the subtropical North Pacific. J. Geophys. Res. **115**, 10.1029/2010jc006507.
---. 2013. Examining the global record of interannual variability in stratification and marine productivity in the low-latitude and mid-latitude ocean. J. Geophys. Res. **118:** 3114-3127, 10.1002/jgrc.20224.
De Boyer Montégut, C., G. Madec, A. Fischer, A. Lazar, and D. Iudicone. 2004. Mixed layer depth over the global ocean: An examination of profile data and a profile-based climatology. J. Geophys. Res. **109**, 10.1029/2004jc002378.
Depauw, F. A., A. Rogato, M. Ribera D'alcala, and A. Falciatore. 2012. Exploring the molecular basis of responses to light in marine diatoms. J. Exp. Bot. **63:** 1575-1591, 10.1093/jxb/ers005.
Deser, C., A. S. Phillips, and M. A. Alexander. 2010. Twentieth century tropical sea surface temperature trends revisited. Geophys. Res. Lett. **37**, 10.1029/2010gl043321.
Durham, W. M., J. O. Kessler, and R. Stocker. 2009. Disruption of vertical motility by shear triggers formation of thin phytoplankton layers. Science **323:** 1067-1070, 10.1126/science.1167334.
Edwards, K. F., M. K. Thomas, C. A. Klausmeier, and E. Litchman. 2012. Allometric scaling and taxonomic variation in nutrient utilization traits and maximum growth rate of phytoplankton. Limnol. Oceanogr. **57:** 554-566, 10.4319/lo.2012.57.2.0554.
Edwards, M., and A. J. Richardson. 2004. Impact of climate change on marine pelagic phenology and trophic mismatch. Nature **430:** 881-884,
Eppley, R. W. 1972. Temperature and phytoplankton growth in the sea. **70:** 1063-1085,
Falkowski, P. G., R. T. Barber, and V. Smetacek. 1998. Biogeochemical controls and feedbacks on ocean primary production. Science **281:** 200-206,
Fleming, S. W. 2010. Signal-to-noise ratios in geophysical and environmental time series. Env. Eng. Geosci. **16:** 389-399,
Follows, M., and S. Dutkiewicz. 2002. Meteorological modulation of the North Atlantic spring bloom. Deep Sea. Res. **49:** 321-344,

700 Garcia, H. E. and others 2010. World Ocean Atlas 2009, Volume 4: Nutrients (phosphate,
701 nitrate, silicate). p. 398. *In* S. Levitus [ed.], NOAA Atlas NESDIS.
702 Hairston, N. G., T. A. Dillon, and B. T. De Stasio. 1990. Field test for the cues of diapause in a
703 freshwater copepod. Ecology **71:** 2218-2223,
704 Hakkinen, S., and P. B. Rhines. 2004. Decline of subpolar North Atlantic circulation during the
705 1990s. Science **304:** 555-559, 10.1126/science.1094917.
706 Hátún, H. and others 2009. Large bio-geographical shifts in the north-eastern Atlantic Ocean:
707 From the subpolar gyre, via plankton, to blue whiting and pilot whales. Prog. Oceanogr.
708 **80:** 149-162, 10.1016/j.pocean.2009.03.001.
709 Hátún, H., A. B. Sando, H. Drange, B. Hansen, and H. Valdimarsson. 2005. Influence of the
710 Atlantic subpolar gyre on the thermohaline circulation. Science **309:** 1841-1844,
711 10.1126/science.1114777.
712 Henson, S., R. Lampitt, and D. Johns. 2012. Variability in phytoplankton community structure in
713 response to the North Atlantic Oscillation and implications for organic carbon flux.
714 Limnol. Oceanogr. **57:** 1591-1601, 10.4319/lo.2012.57.6.1591.
715 Hinder, S. L., G. C. Hays, M. Edwards, E. C. Roberts, A. W. Walne, and M. B. Gravenor. 2012.
716 Changes in marine dinoflagellate and diatom abundance under climate change. Nature
717 Clim. Change **2:** 271-275, 10.1038/nclimate138810.1038.
718 Hurrell, J. W. 1995. Decadal trends in North Atlantic Oscillation: Regional temperature and
719 precipitation. Science **269:** 676-679,
720 Irigoien, X., K. J. Flynn, and R. P. Harris. 2005. Phytoplankton blooms: a 'loophole' in
721 microzooplankton grazing impact? J. Plankton Res. **27:** 313-321, 10.1093/plankt/fbi011.
722 Irigoien, X., J. Huisman, and C. Harris. 2004. Global biodiversity patterns of marine
723 phytoplankton and zooplankton. Nature **429:** 863-866, 10.1038/nature02644.
724 Irwin, A. J., A. M. Nelles, and Z. V. Finkel. 2012. Phytoplankton niches estimated from field
725 data. Limnol. Oceanogr. **57:** 787-797, 10.4319/lo.2012.57.3.0787.
726 Irwin, A. J., and M. J. Oliver. 2009. Are ocean deserts getting larger? Geophys. Res. Lett. **36**,
727 10.1029/2009gl039883.
728 Johnson, C., M. Inall, and S. Häkkinen. 2013. Declining nutrient concentrations in the northeast
729 Atlantic as a result of a weakening Subpolar Gyre. Deep-Sea Res. I. **82:** 95-107,
730 10.1016/j.dsr.2013.08.007.
731 Kalnay, E. and others 1996. The NCEP/NCAR 40-Year Reanalysis Project. Bull. Amer. Met.
732 Soc. **77:** 437-471, 10.1175/1520-0477(1996)077<0437:tnyrp>2.0.co;2.
733 Kenitz, K., R. G. Williams, J. Sharples, Ö. Selsil, and V. N. Biktashev. 2013. The paradox of the
734 plankton: species competition and nutrient feedback sustain phytoplankton diversity.
735 Mar. Ecol. Prog. Ser. **490:** 107-119, 10.3354/meps10452.
736 Kiørboe, T., and A. G. Hirst. 2008. Optimal development time in pelagic copepods. Mar. Ecol.
737 Prog. Ser. **367:** 15-22, 10.3354/meps07572.
738 Kraus, E. B. 1988. Merits and defects of different approaches to mixed layer modeling, p. 37-50.
739 *In* J. C. J. Nihoul and B. M. Jamart [eds.], Small scale turbulence and mixing in the
740 ocean. Elsevier.
741 Landry, M. R., J. Constantinou, M. Latasa, S. L. Brown, R. R. Bidigare, and M. E. Ondrusek.
742 2000. Biological response to iron fertilization in the easter equatorial Pacific (IronEx II).
743 III. Dynamics of phytoplankton growth and microzooplankton grazing. Mar. Ecol. Prog.
744 Ser. **201:** 57-72,

745 Lee, R. F., W. Hagen, and G. Kattner. 2006. Lipid storage in marine zooplankton. Mar. Ecol.
746 Prog. Ser. **307:** 273-306,
747 Lessard, E. J., and M. C. Murrell. 1998. Microzooplankton herbivory and phytoplankton growth
748 in the northwestern Sargasso Sea. Aqua. Micro. Ecol. **16:** 173-188,
749 Leterme, S. C., M. Edwards, L. Seuront, M. J. Attrill, P. C. Reid, and A. W. G. John. 2005.
750 Decadal basin-scale changes in diatom, dinoflagellates, and phytoplankoton color across
751 the North Atlantic. Limnol. Oceanogr. **50:** 1244-1253,
752 Litchman, E., C. A. Klausmeier, O. M. Schofield, and P. G. Falkowski. 2007. The role of
753 functional traits and trade-offs in structuring phytoplankton communities: scaling from
754 cellular to ecosystem level. Ecol. Lett. **10:** 1170-1181, 10.1111/j.1461-
755 0248.2007.01117.x.
756 Lomas, M. W. and others 2010. Increased ocean carbon export in the Sargasso Sea linked to
757 climate variability is countered by its enhanced mesopelagic attenuation. Biogeosci. **7:**
758 57-70,
759 Lozier, M. S., A. C. Dave, J. B. Palter, L. M. Gerber, and R. T. Barber. 2011. On the relationship
760 between stratification and primary productivity in the North Atlantic. Geophys. Res. Lett.
761 **38**, 10.1029/2011gl049414.
762 Margalef, R. 1978. Life-forms of phytoplankton as survival alternatives in an unstable
763 environment. Ocean. Acta **1:** 493-509,
764 Marshall, J. and others 2001. North Atlantic climate variability: phenomena, impacts and
765 mechanisms. Int. J. Clim. **21:** 1863-1898, 10.1002/joc.693.
766 Menzel, D. W., and J. H. Rhyther. 1960. The annual cycle of primary production in the Sargasso
767 Sea off Bermuda. Deep-Sea Res. **6:** 351-367,
768 Neuer, S. and others 2002. Differences in the biological carbon pump at three subtropical ocean
769 sites. Geophys. Res. Lett. **29**, 10.1029/2002gl015393.
770 Niiler, P. P., and E. B. Kraus. 1977. One-dimensional models of the upper ocean, p. 143-172. *In*
771 E. B. Kraus [ed.], Modeling and prediction of the upper layers of the ocean. Pergamon.
772 Oschlies, A. 2001. NAO-induced long-term changes in nutrient supply to the surface waters of
773 the North Atlantic. Geophys. Res. Lett. **28:** 1751-1754, 10.1029/2000gl012328.
774 Palter, J. B., and M. S. Lozier. 2008. On the source of Gulf Stream nutrients. J. Geophys. Res.
775 **113**, 10.1029/2007jc004611.
776 Polovina, J. J., E. A. Howell, and M. Abecassis. 2008. Ocean's least productive waters are
777 expanding. Geophys. Res. Lett. **35**, 10.1029/2007gl031745.
778 Raitsos, D. E., P. C. Reid, S. J. Lavender, M. Edwards, and A. J. Richardson. 2005. Extending
779 the SeaWiFS chlorophyll data set back 50 years in the northeast Atlantic. Geophys. Res.
780 Lett. **32**, 10.1029/2005gl022484.
781 Richardson, A. J. and others 2006. Using continuous plankton recorder data. Prog. Oceanogr. **68:**
782 27-74, 10.1016/j.pocean.2005.09.011.
783 Rose, J. M., and D. A. Caron. 2007. Does low temperature constrain the growth rates of
784 heterotrophic protists? Evidence and implications for algal blooms in cold waters.
785 Limnol. Oceanogr. **52:** 886-895,
786 Rykaczewski, R. R., and J. P. Dunne. 2010. Enhanced nutrient supply to the California Current
787 Ecosystem with global warming and increased stratification in an earth system model.
788 Geophys. Res. Lett. **37**, L21606, doi:10.1029/2010GL045019.
789 Rynearson, T. A. and others 2013. Major contribution of diatom resting spores to vertical flux in
790 the sub-polar North Atlantic. Deep-Sea Res. I **82:** 60-71, 10.1016/j.dsr.2013.07.013.

Sarthou, G., K. R. Timmermans, S. Blain, and P. Tréguer. 2005. Growth physiology and fate of diatoms in the ocean: a review. J. Sea Res. **53:** 25-42, 10.1016/j.seares.2004.01.007.

Schartau, M., M. R. Landry, and R. A. Armstrong. 2010. Density estimation of plankton size spectra: a reanalysis of IronEx II data. J. Plankton Res. **32:** 1167-1184, 10.1093/plankt/fbq072.

Sen, P. K. 1968. Estimates of the regression coefficient based on Kendall's Tau. J. Amer. Stat. Soc. **63:** 1379-1389,

Sieracki, M. E., P. G. Verity, and D. K. Stoecker. 1993. Plankton community response to sequential silicate and nitrate depletion during the 1989 North Atlantic spring bloom. Deep Sea Res. II **40:** 213-225, 10.1016/0967-0645(93)90014-e.

Smayda, T. J. 1997. Harmful algal blooms: their ecophysiology and general relevance to phytoplankton blooms in the sea. Limnol. Oceanogr. **42:** 1137-1153,

Smayda, T. J., and C. S. Reynolds. 2001. Community assembly in marine phytoplankton: application of recent models to harmful dinoflagellate blooms. J. Plankton Res. **23:** 447-461,

Smith, D., and J. Murphy. 2007. An objective ocean temperature and salinity analysis using covariances from a global climate model. J. Geophys. Res. **112**, 10.1029/2005JC003172.

Sommer, U. 1985. Seasonal succession of phytoplankton in Lake Constance. BioSci. **35:** 351-357,

Steinacher, M. and others 2010. Projected 21st century decrease in marine productivity: a multi-model analysis. Biogeosci. **7:** 979-1005,

Steinberg, D. K., C. A. Carlson, N. R. Bates, R. J. Johnson, A. Michaels, and A. H. Knap. 2001. Overview of the US JGOFS Bermuda Atlantic Time-series Study (BATS): a decade-scale look at ocean biology and biogeochemistry. Deep Sea Res II **48:** 1405-1447,

Stoecker, D. K. 1999. Mixotrophy among dinoflagellates. J. Eukaryot. Microbiol. **46:** 397-401,

Sverdrup, H. 1953. On conditions of the vernal blooming of phytoplankton. J. Con. Int. Exp. Mer **18:** 287-295,

Taboada, F. G., and R. Anadon. 2014. Seasonality of North Atlantic phytoplankton from space: impact of environmental forcing on a changing phenology (1998-2012). Glob. Change Biol. **20:** 698-712, 10.1111/gcb.12352.

Tarran, G. A., J. L. Heywood, and M. V. Zubkov. 2006. Latitudinal changes in the standing stocks of nano- and picoeukaryotic phytoplankton in the Atlantic Ocean. Deep-Sea Res. II **53:** 1516-1529, 10.1016/j.dsr2.2006.05.004.

Taylor, A. H., D. S. Harbour, R. P. Harris, P. H. Burkill, and E. S. Edwards. 1993. Seasonal succession in the pelagic ecosystem of the North Atlantic and the utilization of nitrogen. J. Plankton Res. **15:** 875-891,

Taylor, G. T. and others 2012. Ecosystem responses in the southern Caribbean Sea to global climate change. Proc. Natl. Acad. Sci. U S A **109:** 19315-19320, 10.1073/pnas.1207514109.

Taylor, J. R., and R. Ferrari. 2011. Shutdown of turbulent convection as a new criterion for the onset of spring phytoplankton blooms. Limnol. Oceanogr. **56:** 2293-2307, 10.4319/lo.2011.56.6.2293.

Theil, H. 1950. A rank-invariant method of linear and polynomial regression analysis. Proc. Royal Neth. Acad. Sci. **LIII:** 1397-1412,

Uitz, J., H. Claustre, A. Morel, and S. B. Hooker. 2006. Vertical distribution of phytoplankton communities in open ocean: An assessment based on surface chlorophyll. J. Geophys. Res. **111**, C08005, doi:10.1029/2005JC003207.

Ward, B. A., S. Dutkiewicz, A. D. Barton, and M. J. Follows. 2011. Biophysical aspects of resource acquisition and competition in algal mixotrophs. Am. Nat. **178:** 98-112, 10.1086/660284.

Ward, B. A., S. Dutkiewicz, O. Jahn, and M. J. Follows. 2012. A size-structured food-web model for the global ocean. Limnol. Oceanogr. **57:** 1877-1891, 10.4319/lo.2012.57.6.1877.

Williams, R. G., and M. J. Follows. 1998. The Ekman transfer of nutrients and maintenance of new production over the North Atlantic. Deep-Sea Res. I. **45:** 461-489,

---. 2011. Ocean Dynamics and the Carbon Cycle. Cambridge University Press.

Williams, R. G., A. J. Mcclaren, and M. J. Follows. 2000. Estimating the convective supply of nitrate and implied variability in export production over the North Atlantic. Global Biogeochem. Cyc. **14:** 1299-1313,

Williams, R. G. and others 2011. Nutrient streams in the North Atlantic: Advective pathways of inorganic and dissolved organic nutrients. Global Biogeochem. Cyc. **25**, 10.1029/2010gb003853.

Williams, R. G., V. Roussenov, and M. J. Follows. 2006. Nutrient streams and their induction into the mixed layer. Global Biogeochem. Cyc. **20**, 10.1029/2005gb002586.

Tables

Table 1: Pooled variance for ecological and physical time series describing the original observations (Absolute values; *PCI*), the long-term trend (PCI^{Trend}), the seasonal cycle (PCI^{Season}), and the detrended anomalies (PCI^{Var}). The pooled variance is a weighted, spatial average of the temporal variance at each location, where the weights are the number of monthly observations. Values have been normalized by the pooled variance in the seasonal cycle, such that seasonal cycle values are 1 and values are unitless. Values greater than 1 indicate greater variance than in the seasonal cycle.

	Absolute values	**Long-term trend**	**Seasonal Cycle**	**Detrended anomalies**
PCI	3.039	0.130	1.000	1.999
Diatoms	3.374	0.274	1.000	2.345
Dinoflagellates	4.771	0.093	1.000	3.450
Wind speed	1.602	0.002	1.000	0.599
Heat flux	1.122	0.001	1.000	0.120
SST	1.053	0.004	1.000	1.048

Figures legends

Figure 1. (A) Ekman upwelling velocity (w_{ek}; m yr^{-1}) in downwelling ($w_{ek} < 0$) subtropical and upwelling ($w_{ek} > 0$) subpolar gyres in the North Atlantic. The black contours indicate the annual mean nitrate concentration at the surface (μmol l^{-1}). (B) Mean nitrate concentration (μmol l^{-1}) with depth in the subtropical (red lines, 'ST' on map) and subpolar (blue lines, 'SP' on map) gyres for August (dashed line) and February (solid line). Mixed layer depths in February (F, deeper) and August (A, shallower) are shown at right. Ekman upwelling velocity is calculated using NCEP/NCAR annual mean wind stress data (Kalnay et al. 1996) following Williams and Follows (Williams and Follows 2011). Monthly mean nitrate data are taken from the World Ocean Atlas (Garcia et al. 2010) and averaged over 5°x5° area.

Figure 2. (A) Log_{10} total number of raw CPR samples taken within each 2.5°x2.5° grid cell during 1958-2006. Log_{10} annual mean (B) PCI, (C) total diatoms, and (D) total dinoflagellates.

Figure 3. (A) Absolute value PCI time series in the western English Channel (49.4° N, 5° W) for 1990-2000, with climatological seasonal cycle (PCI^{Season}) inset. (B) PCI monthly anomalies (PCI') with seasonal cycle subtracted and long term trend overlaid (PCI^{Trend}), (C) detrended anomaly time series (PCI^{Var}), and (D) estimate of sampling noise (PCI^{Noise}) for 1958-2006. The example noise time series is created by multiplying the standard error by a randomly generated Gaussian white noise time series.

Figure 4. Kendall's τ correlation between the climatological mean seasonal cycles of PCI (PCI^{Season}; A), summed diatoms (Dia^{Season}; B), and summed dinoflagellates ($Dino^{Season}$; C) and,

893 from top to bottom down each column, climatological seasonal cycles of surface wind speed,
894 total heat flux, turbulent kinetic energy (TKE) generation, mixed layer depth (MLD),
895 stratification, and sea surface temperature (SST). Only significant correlations (p<0.05) are
896 shown. The dashed black contour shows the approximate boundary between the subpolar and
897 subtropical gyres, as defined by the 4 μmol l^{-1} mean annual surface nitrate contour. Nitrate data
898 from the World Ocean Atlas 2009 (Garcia et al. 2010).
899
900 Figure 5. Climatological seasonal cycles of PCI (solid line), diatom abundance (dotted line),
901 dinoflagellate abundance (dashed line), and mixed layer depth (solid line with filled circles; scale
902 inverted to show negative depths) in subtropical (A) and subpolar (B) locations noted in Fig. 1
903 (averaged over a 10°x10° area). The vertical gray line shows when heat fluxes switch from
904 cooling to heating the ocean surface in spring. We have included in shaded gray the 95%
905 confidence interval for PCI (±2σ, where σ is the monthly standard error).
906
907 Figure 6. Linear trends, indicated by the Kendall's τ coefficient, in (A) CPR metrics, (B)
908 atmospheric forcing, and (C) surface ocean conditions over 1958-2006. Only significant
909 correlations (p<0.05) are shown. The dashed black perimeter in the biological trends at left
910 indicates where CPR data are available.
911
912 Figure 7. Kendall's τ correlation between absolute value (*PCI*; A), climatological mean seasonal
913 cycle (PCI^{Season}; B), and detrended PCI anomaly (PCI^{Var}; C) time series and corresponding
914 surface wind speed, total heat flux, TKE generation, mixed layer depth (MLD), stratification, and
915 sea surface temperature (SST) time series. Only significant correlations (p<0.05) are shown.

916 Data in column B are the same as Fig. 3A, but are repeated to show the progression and strength
917 of correlation at each timescale.
918
919 Figure 8. Detrended anomaly time series (indicated by the "Var" superscript) for PCI (solid line),
920 diatom abundance (dotted line), dinoflagellate abundance (dashed line), and mixed layer depth
921 (solid line with filled circles) in subtropical (A) and subpolar (B) locations noted in Fig. 1
922 (annually averaged over a 10°x10° area). Positive MLD anomalies indicate deeper MLDs. We
923 have included in shaded gray the 95% confidence interval for PCI (±2σ, where σ is the standard
924 error of all anomalies within the region over a year).
925
926 Figure 9. (A) Signal variance for absolute value (*PCI*; top) and detrended PCI anomaly (PCI^{Var};
927 middle) time series, normalized by the noise variance (PCI^{Noise}; bottom) to calculate the signal to
928 noise ratio (B). Signal variance and signal-to-noise ratio are presented in $\log_{10}$ units; values
929 greater than 1 (i.e., 10^0) indicate ecological variability above and beyond our estimate of CPR
930 sampling noise.
931
932
933
934
935
936

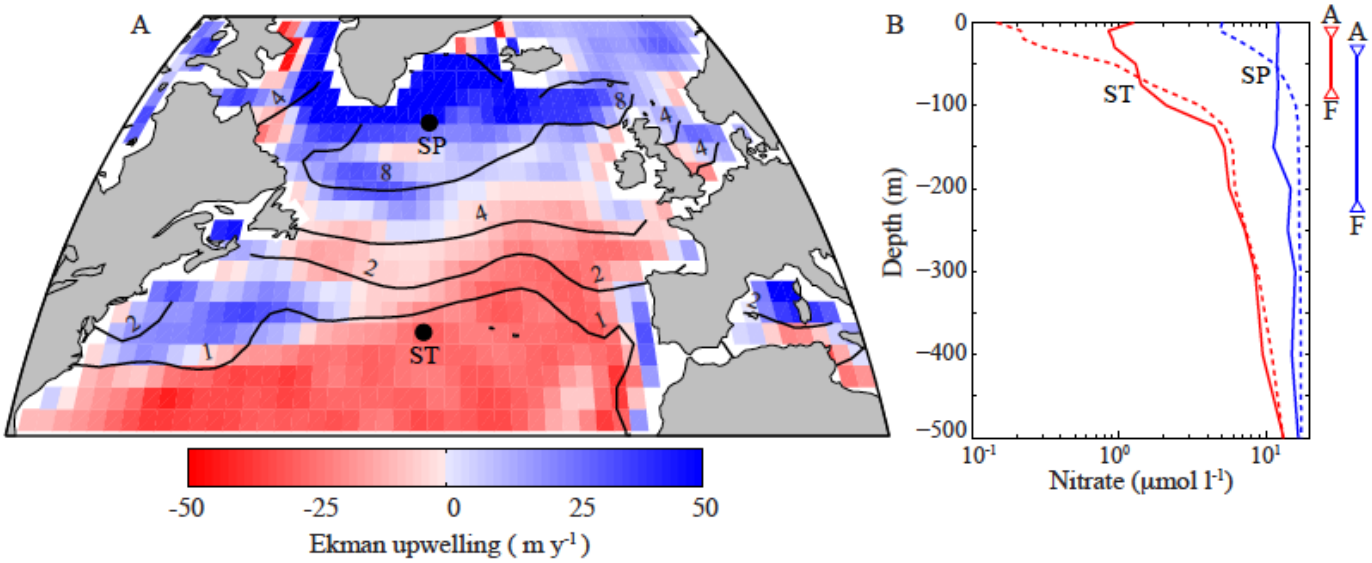
A
SP
ST
8
4
2
1
-50
-25
0
25
50
Ekman upwelling (m y-1)
B
0
−100
−200
−300
−400
−500
Depth (m)
SP
ST
10-1
100
101
Nitrate (µmol l-1)
A
F
A
F

Figure 1

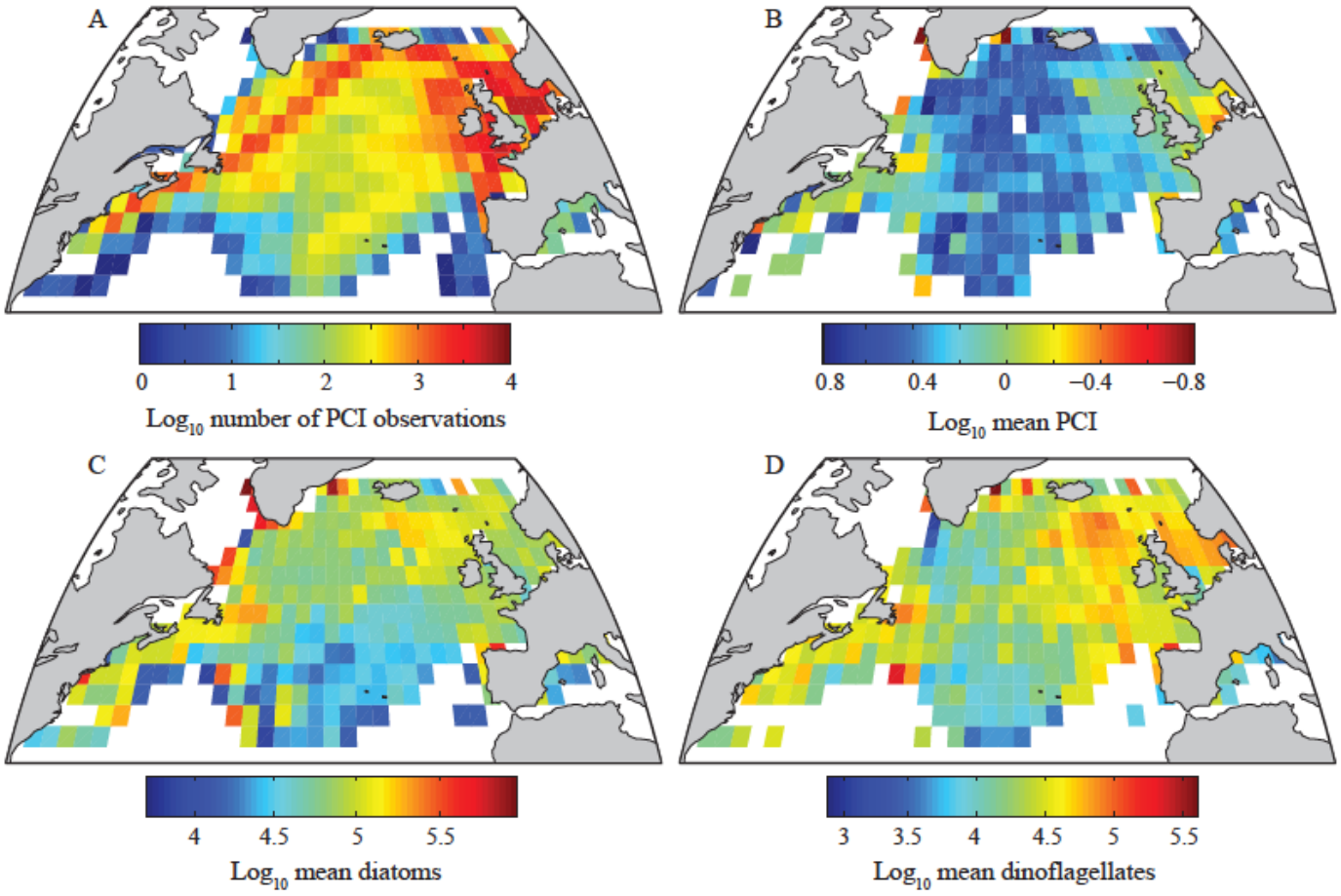
A
0
1
2
3
4
Log10 number of PCI observations
B
0.8
0.4
0
−0.4
−0.8
Log10 mean PCI
C
4
4.5
5
5.5
Log10 mean diatoms
D
3
3.5
4
4.5
5
5.5
Log10 mean dinoflagellates

Figure 2

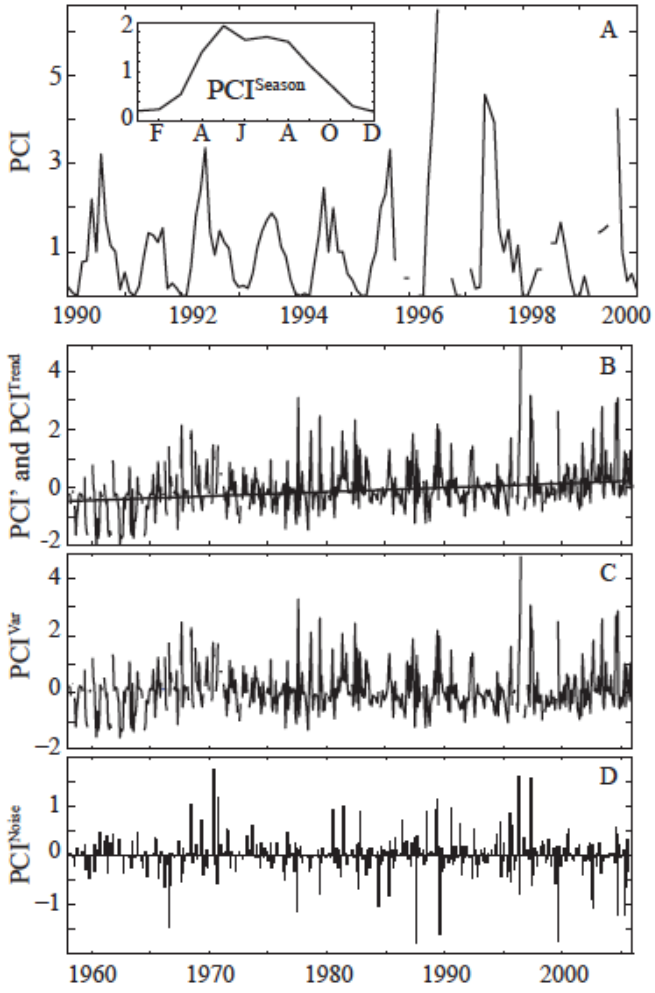
A
PCI
PCI^Season
F A J A O D
1990 1992 1994 1996 1998 2000
B
PCI' and PCI^Trend
C
PCI^Var
D
PCI^Noise
1960 1970 1980 1990 2000

Figure 3

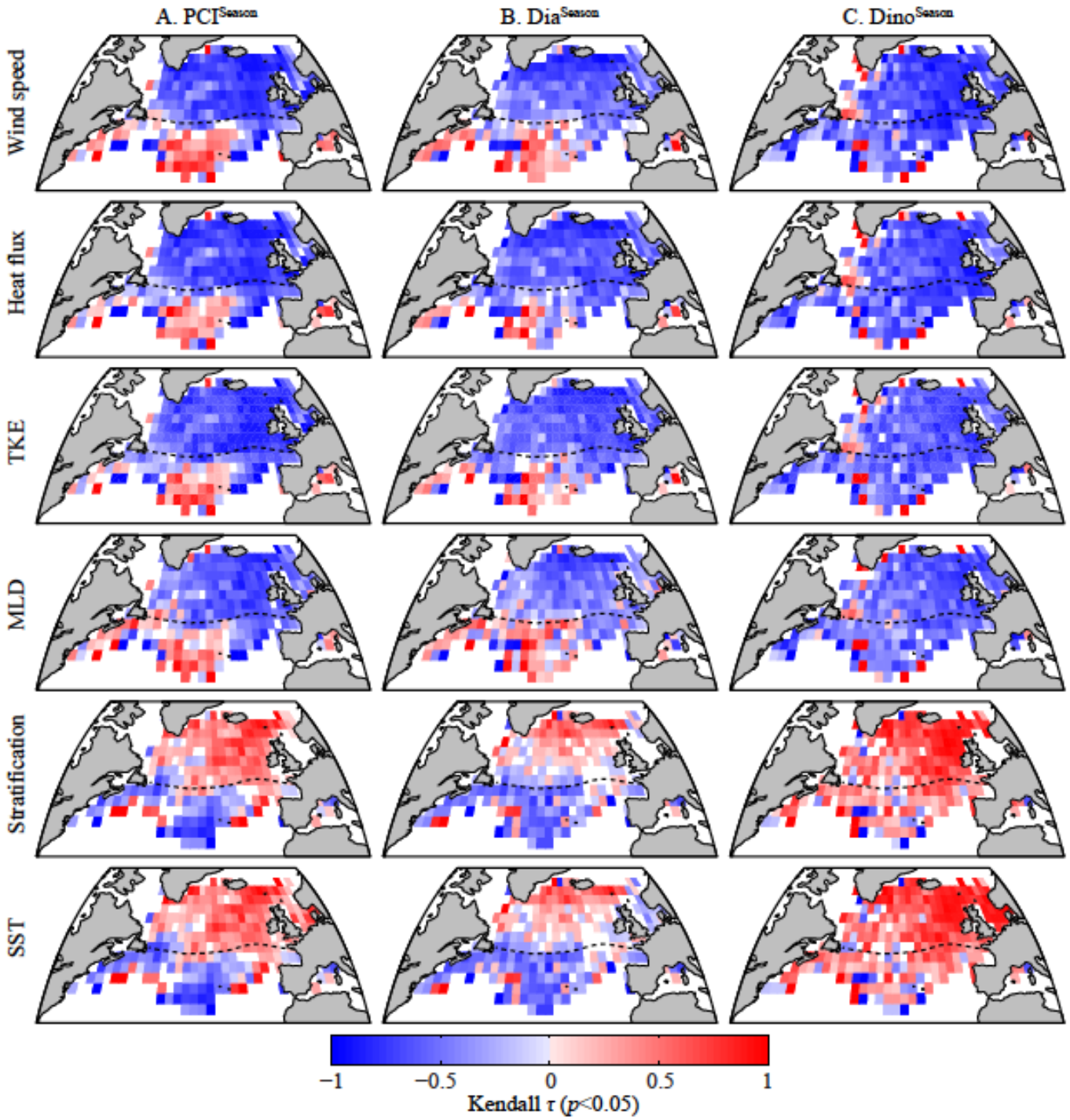
A. PCI^Season
B. Dia^Season
C. Dino^Season
Wind speed
Heat flux
TKE
MLD
Stratification
SST
−1
−0.5
0
0.5
1
Kendall τ (p<0.05)

Figure 4

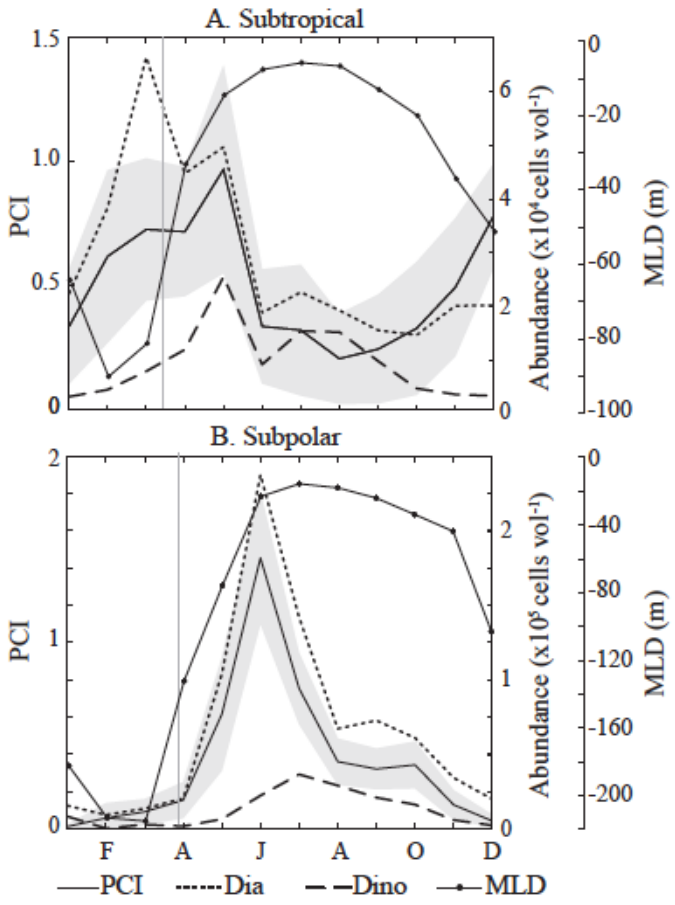
A. Subtropical
B. Subpolar
PCI
Abundance (x10⁴cells vol⁻¹)
Abundance (x10⁵ cells vol⁻¹)
MLD (m)
F
A
J
A
O
D
PCI
Dia
Dino
MLD

Figure 5

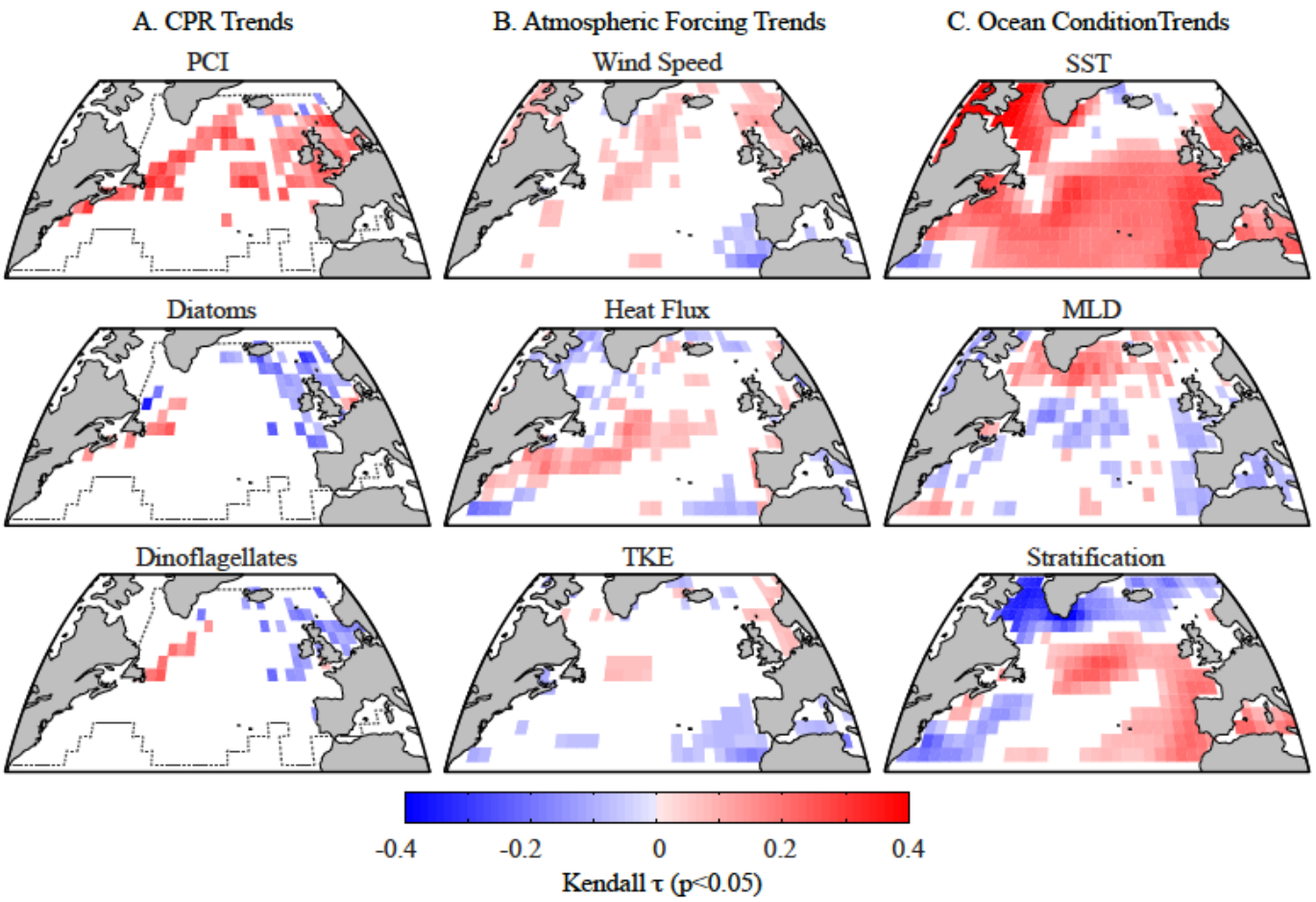
A. CPR Trends
PCI
B. Atmospheric Forcing Trends
Wind Speed
C. Ocean ConditionTrends
SST
Diatoms
Heat Flux
MLD
Dinoflagellates
TKE
Stratification
-0.4
-0.2
0
0.2
0.4
Kendall τ (p<0.05)

Figure 6

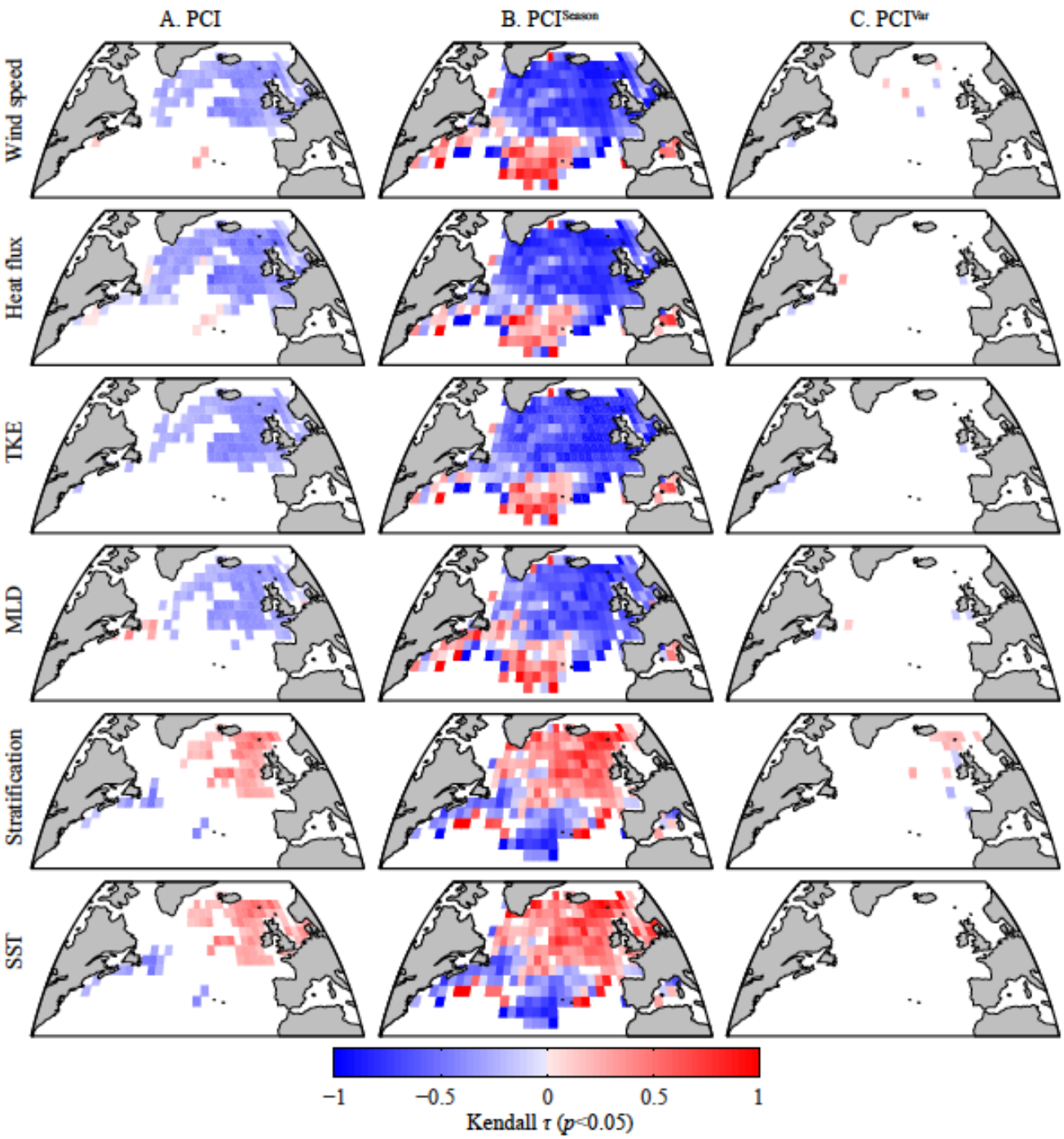
A. PCI
B. PCI^Season
C. PCI^Var
Wind speed
Heat flux
TKE
MLD
Stratification
SST
−1
−0.5
0
0.5
1
Kendall τ (p<0.05)

Figure 7

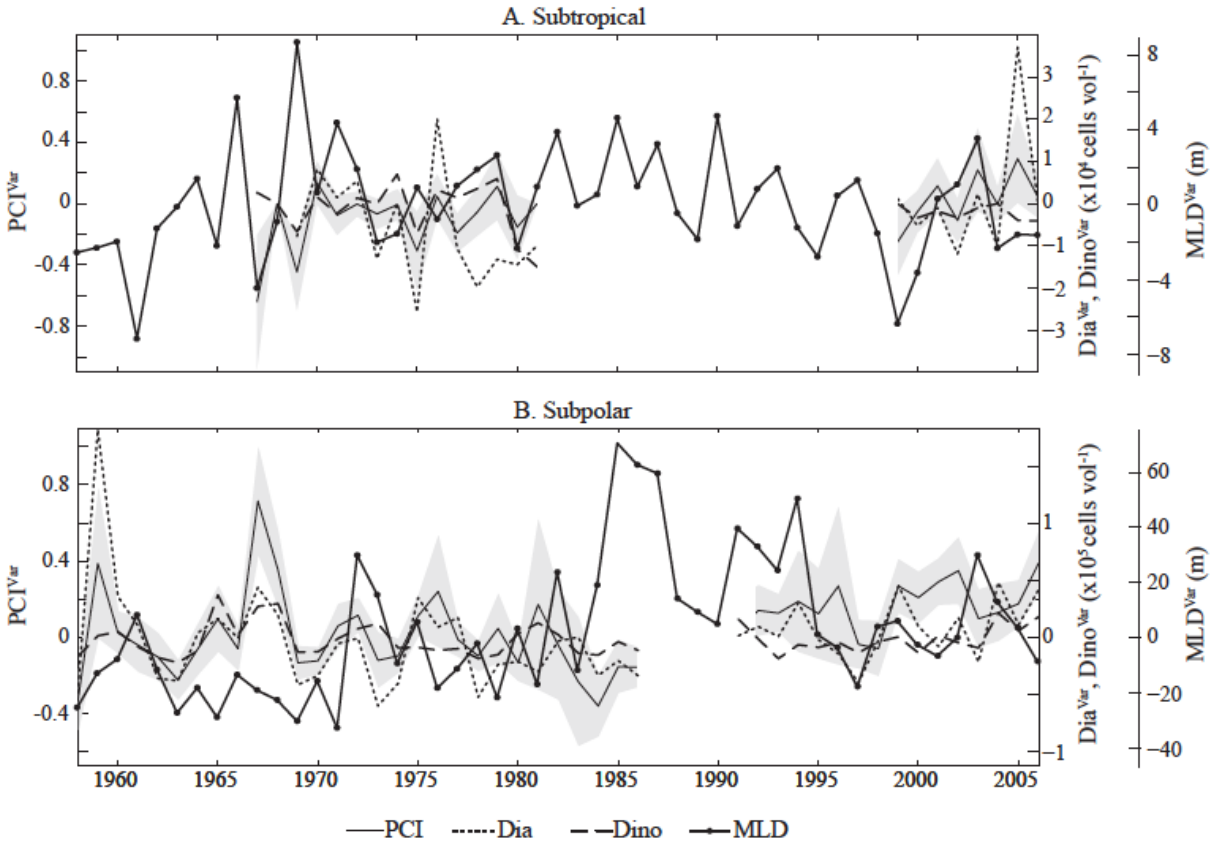
A. Subtropical
B. Subpolar
PCI^Var
Dia^Var, Dino^Var (x10^4 cells vol^-1)
MLD^Var (m)
Dia^Var, Dino^Var (x10^5 cells vol^-1)
1960
1965
1970
1975
1980
1985
1990
1995
2000
2005
PCI
Dia
Dino
MLD

Figure 8

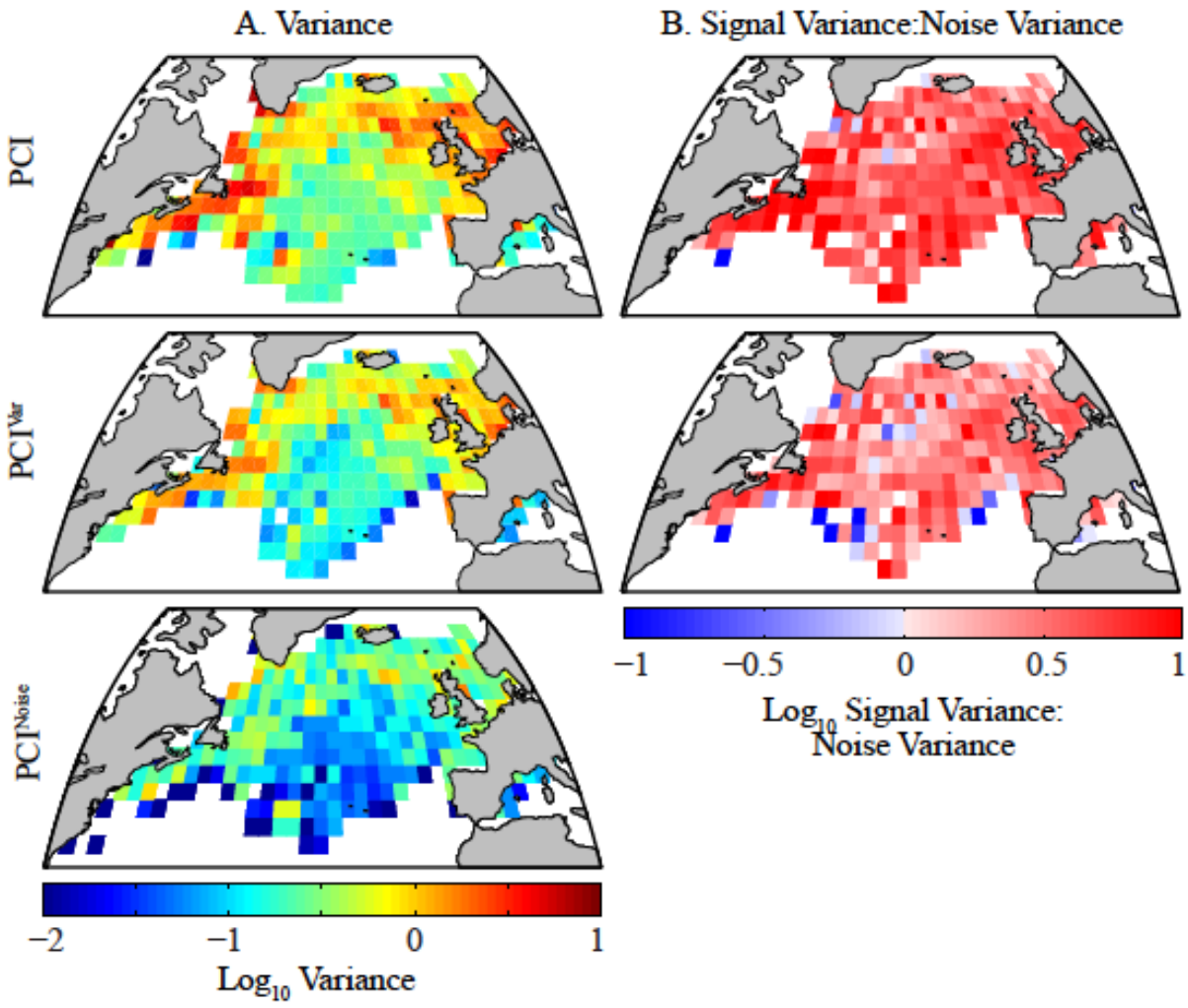
A. Variance
B. Signal Variance:Noise Variance
PCI
PCI^Var
PCI^Noise
−2
−1
0
1
Log10 Variance
−1
−0.5
0
0.5
1
Log10 Signal Variance:
Noise Variance

Figure 9